ORIGINAL PAPER

A signal-off photoelectrochemical aptasensor for ultrasensitive 17β-estradiol detection based on rose-like CdS@C nanostructure and enzymatic amplification

Lian-Hong Tu[1] · Jian-Hong Zhu[1] · Aisyah-protonia Tanjung[1] · Min Wang[1] · Jinwei Kang[1] · Ai-Jun Wang[1] · Li-Ping Mei[1] · Yadong Xue[2] · Pei Song[2]

Abstract

Carbon-coated cadmium sulfide rose-like nanostructures (CdS@C NRs) were prepared via a facile solvothermal approach and used as the photoelectrochemical (PEC) sensing platform for the integration of functional biomolecules. Based on this, a novel "signal-off" PEC aptasensor mediated by enzymatic amplification was proposed for the sensitive and selective detection of 17β-estradiol (E2). In the presence of E2, alkaline phosphatase-modified aptamer (ALP-apta) were released from the electrode surface through the specific recognition with E2, which caused the negative effect on PEC response due to the decrease of ascorbic acid (AA) produced by the ALP in situ enzymatic catalysis. The developed PEC aptasensor for detection of E2 exhibited a wide linear range of 1.0–250 nM, with the low detection limit of 0.37 nM. This work provides novel insight into the design of potential phoelectroactive materials and the application of signal amplification strategy in environmental analysis field.

Introduction

17β-Estradiol (E2), as a typical endogenous estrogen, can not only affect people and animal sex differentiation, and normal metabolic function, but also disturb the normal growth, development, and reproduction of the organism [1]. Fatally, E2 in the environment can be harmful to organisms

Lian-Hong Tu and Jian-Hong Zhu contributed equally to this work.

✉ Li-Ping Mei
mei.lp@zjnu.edu.cn

✉ Yadong Xue
xueyadong@zju.edu.cn

✉ Pei Song
ppsong2020@outlook.com

[1] College of Geography and Environmental Sciences, College of Chemistry and Life Sciences, Zhejiang Normal University, Jinhua 321004, China

[2] Central Laboratory, Affiliated Jinhua Hospital, Zhejiang University School of Medicine, Jinhua 321000, China

even at very low concentrations (ng L^{-1}) [2]. Hence, it is critically significant to establish an effective, rapid assay for E2 in the environmental and biological analysis field.

Currently, numerous endeavors have focused on the development of effective E2 assay methods, including spectrometry [3], colorimetry [4], immunoassay [5], fluorescence [6], and electrochemistry (EC) [7]. Although these analytical methods have achieved satisfied results, they still present several obstacles in practical applications, such as expensive device, time-consuming process, technical complexity, or limited sensitivity [8]. Therefore, it still remains a grand challenge to develop a facile, sensitive, and accurate analytical method for E2 assay.

As an emerging technology, photoelectrochemical (PEC) sensors have aroused intense interest among researchers due to its easy miniaturization, low background signal, and fast response [9–13]. Nevertheless, low sensitivity and selectivity of PEC sensors have hindered its further application in environmental analysis [14–17]. Design of efficient photoelectroactive materials is a pivotal issue in the construction of PEC sensor with excellent sensitivity. Cadmium sulfide (CdS), as significant semiconductor, has commonly used

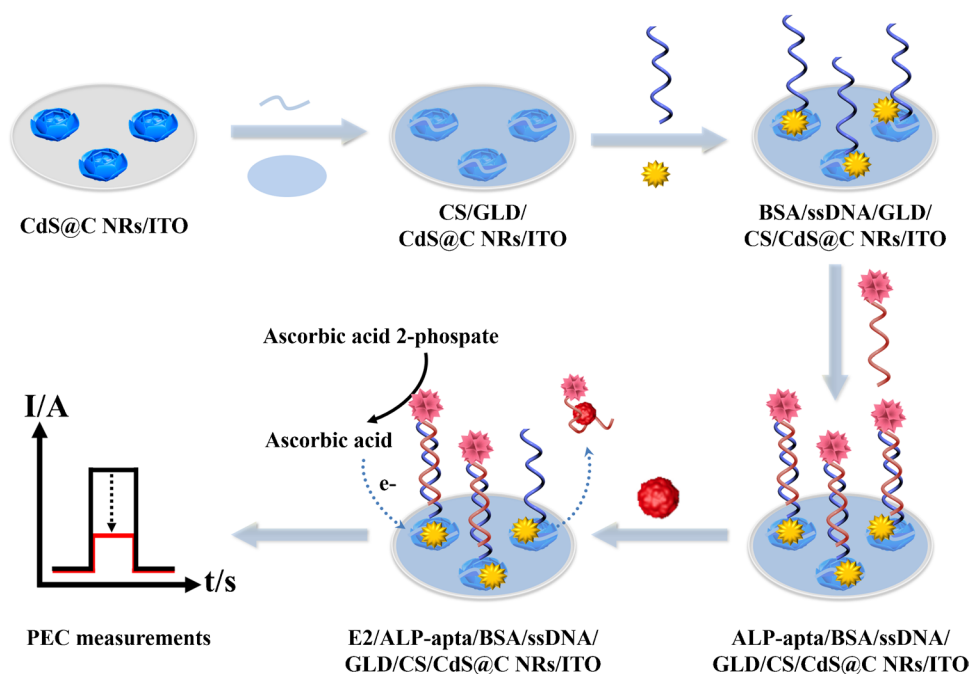**Scheme 1** Schematic diagram of sensitive PEC biosensor for assay of E2

in photocatalysis, PEC sensors, and photodegradation, and demonstrated outstanding photocatalytic performance under visible light irradiation [18–20]. Unfortunately, CdS-based photoelectroactive materials suffer from several inherent disadvantages of easy aggregation and photocorrosion, which substantially hamper their extensive application [20]. Integration carbon layer and CdS is one of the most effective surface modification method to solve the above drawbacks of CdS. Introduction of carbon layer can stabilize the surface of CdS and suppress its photocorrosion behavior. Importantly, the photoelectrochemical properties of CdS after modification of coated carbon have been markedly improved and served as potential photoelectric materials. For instance, Hu et al. synthesized carbon-coated CdS with superior photostability, revealing remarkable photocatalytic activity during pollutant degradation process [19].

Biological recognition process is also of great importance for the PEC biosensing system to acquire exceptional selectivity. Aptamer can be commonly regarded as a new molecular identification element to selectively recognize various targets due to its high affinity and specificity [21, 22]. Furthermore, aptamers have demonstrated to be more promising in sensors compared with antibodies, owing to their stability, easy synthesis, facile modification, and relatively low cost [21]. Combined with the readily chemical modification characteristic of aptamer, devising signal amplification strategies is another critical to improve the sensitivity of PEC sensors. Among diverse signal amplification strategies, enzyme-mediate signal amplification gained broad attention due to its advantages of exceptional efficiency, and exquisite selectivity. For example, Ai's group reported a novel PEC biosensor with high sensitivity for protein kinase A activity detection based on signal amplification of alkaline phosphatase (ALP) [23].

In this work, an ultrasensitive "signal-off" PEC aptasensor for assay of E2 was constructed based on carbon-coated cadmium sulfide rose-like nanostructures (CdS@C NRs), assisted with ALP-mediated signal amplification strategy. As depicted in Scheme 1, the single-stranded DNA was firstly modified on the electrode surface, while the ALP-modified E2 aptamer (ALP-apta) was bonded to the ssDNA via base complementary pairing. In the absence of E2, the enhanced photocurrent of CdS@C NRs was achieved due to the in situ generation of electron donor (ascorbic acid, AA), which was triggered by ALP-mediated hydrolysis reaction. With the addition of E2, ALP-apta were released from the electrode surface after the specific recognition with E2, causing the negative effect on PEC response. Accordingly, this protocol indicated the "signal-off" photocurrent response with increases in concentrations of E2. The developed PEC aptasensor reveals high selectivity and excellent sensitivity for E2 assay in the real samples.

Experimental

Materials and instruments

Experimental materials and characterization instruments are provided in detail in Electronic Supplementary Material (ESM).

Synthesis of CdS@C NRs

CdS@C NRs was prepared using a facile solvothermal process. Typically, 0.6851 g of $CdCl_2 \cdot 2.5H_2O$, 0.4476 g of D-penicillamine, 0.4280 g of glucose, and 0.3330 g of polyvinylpyrrolidone (PVP; MW ~ 58 K) were sequentially dissolved in 30 mL of ethylene glycol (EG) under sonication condition. The resulting homogeneous solution was then transferred into a 50-mL Teflon-lined stainless-steel autoclave and kept for 12 h at 160 °C. After cooling down to room temperature, the samples were collected by centrifugation, and sufficiently washed with anhydrous ethanol and distilled water, subsequently dried at 60 °C for further use.

Construction of the aptasensor

For the construction of PEC aptasensor, 20 µL of 2.0 mg mL^{-1} CdS@C NRs was modified on indium tin oxide (ITO) surface (diameter = 5.0 mm). To ensure that the -NH$_2$-modified ssDNA could be linked on the surface of the above electrode, chitosan (CS) and glutaraldehyde (GLD) were progressively coated on the electrode. Twenty microliters of 0.02 wt% chitosan (CS) solution was dropped and then dried at 40 °C for 1 h. Twenty microliters of 5.0 wt% glutaraldehyde (GLD) solution was introduced and incubated for 1 h in the dark, followed by incubation with NH$_2$ modified ssDNA (1.0 µM, 20 µL) at 4 °C overnight. The electrode was subsequently cultured with 10 µL BSA solution (1.0 wt%) at 37 °C for 1 h to block non-specific binding sites. Afterwards, 20 µL of ALP-modified aptamer (2.0 µM) was added to the above electrode and reacted with the ssDNA at 37 °C for 2 h to form double-strand DNA by hybridization. Notably, during the preparing progress, the electrode was extensively rinsed with phosphate buffer solution (PBS, pH 7.4, 10 mM) after each modification step to remove the residual reagent. At last, the prepared electrode was stored at 4 °C for further use.

PEC assay

For E2 analysis, different concentrations of E2 (20 µL) were introduced and reacted with the developed aptasensor at 37 °C for 40 min. Then, the aptasensor was immersed into 2.5 mM L-ascorbic acid 2-phosphate solution (AAP, 4 mL) for 1 h at 37 °C. Eventually, the PEC measurements were performed on the PEC measurement system, which consist of a CHI 660A electrochemical workstation and a PEC light source system at a constant bias of 0 V, by using PBS (pH 8.0) as the electrolyte.

Results and discussion

Characterization of as-synthesized samples

In this study, CdS rose-like nanostructures coated with a thin carbon layer (CdS@C NRs) were prepared using a facile solvothermal method and served as the platform of the aptasensor. The scanning electron microscope (SEM) images show the rose-like nanostructure of the samples with uniform size of about 586 nm (Fig. 1A–B). These rose-like nanostructures are mainly composed of multiple petal-like units with polygonal shape, which afford the large surface area for the immobilization of biomolecules. As shown in Fig. 1C, rose-like nanostructure assembled by irregular polygonal shape is further elucidated by transmission electron microscopy (TEM), which is consistent with the SEM results. As observed from high-resolution TEM (HR-TEM), the calculated lattice spacing of different regions are 0.322 nm and 0.362 nm, corresponding to the (101) and (100) crystal planes of CdS particle [24], respectively. Additionally, an amorphous carbon layer with thickness of 4.77 nm is observed outside of CdS surface (Fig. 1D). The polycrystalline structure of the samples is demonstrated by the selected area electron diffraction (SAED, Fig. 1E).

The crystal structure of CdS@C NRs was identified by X-ray diffraction (XRD) analysis. As depicted in Fig. 1F, there are several obvious characteristic diffraction peaks at 24.8°, 26.5°, 28.2°, 36.6°, 43.7°, 47.8°, and 51.8°, corresponding to (100), (002), (101), (102), (110), (103), and (112) planes of the CdS (JCPDS No. 41–1049), respectively [24]. No peak corresponding to the carbon layer is observed for the as-synthesized carbon coated samples, which may be due to the existence of ultrathin or amorphous carbon layer, and the possible peaks overlap for carbon materials and CdS at 26° [18].

X-ray photoelectron spectroscopy (XPS) was used to study the chemical state and chemical composition of CdS@C NRs. Survey XPS spectrum of the sample confirmed the existence of Cd, S, C, and O elements (Fig. 2A). The high-resolution Cd 3d XPS spectrum shows two obvious characteristic peaks at 411.4 eV and 404.7 eV attributing to Cd 3d$_{3/2}$ and Cd 3d$_{5/2}$, respectively, which prove the presence of Cd^{2+} species (Fig. 2B) [25]. There were two characteristic peaks at 161.0 eV and 162.3 eV of S 2p assigning to S 2p$_{3/2}$ and S 2p$_{1/2}$, indicating the existence of S^{2-} species (Fig. 2C) [26]. As seen in Fig. 2D, the C 1 s peak can also be divided into two separate peaks. The C 1 s peak at 284.7 eV and 287.5 eV belong to sp^2-carbon material (C=C) and oxygen-containing carbon material (C=O), respectively [27]. These XPS results further attest the co-existence of carbon layer and CdS in the prepared samples.

Fig. 1 **A–B** SEM images. **C-D** Low- and high-resolution TEM images. **E** SAED image. **F** XRD pattern of CdS@C NRs. Inset in **A** shows the particle-size distribution
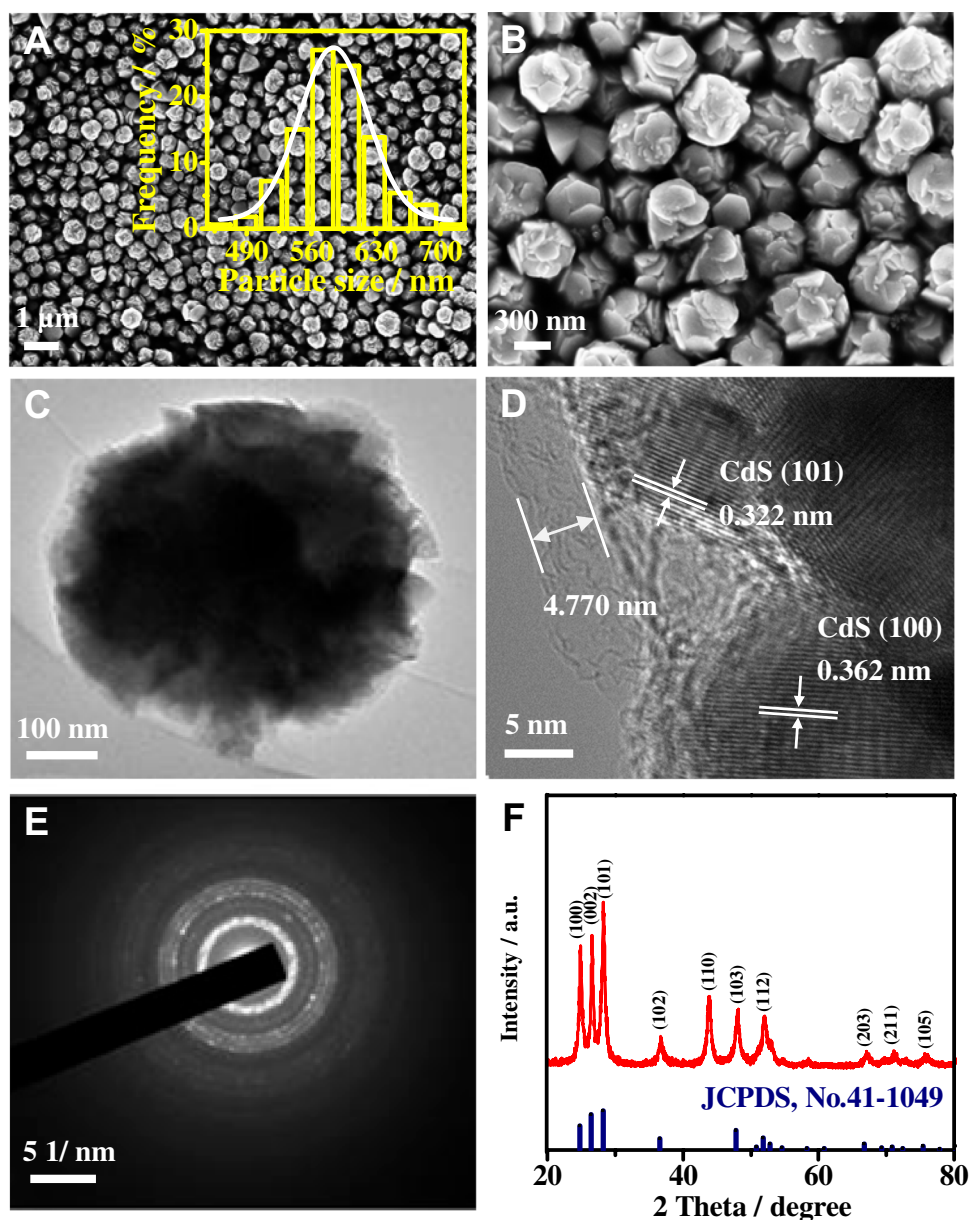
UV–vis diffuse reflection spectrum (DRS) analysis was performed to investigate the optical properties of CdS@C NRs (Fig. 2E). The CdS@C NRs display a wide UV–vis absorption in the range of 300~550 nm. The band gap of CdS@C NRs can be calculated to be 2.07 eV based on the UV–vis DRS (Fig. 2F) [28], which is narrower in contrast with pure CdS nanoparticles (2.4 eV) due to the modification of carbon layer [20].

The possible electron transfer mechanism was proposed on the basis the above results, shown in Scheme 2. Under illumination, amorphous surface carbon of CdS@C NRs can absorb visible light, and then the excited electrons of CdS transfer from valence band to conduction band, producing electron–hole (e^-/h^+) pairs. More importantly, the coated carbon species of CdS@C NRs can effectively promote the electron transfer and inhibit recombination of photoexcited e^-/h^+ pairs [29]. Simultaneously, in situ generated AA can be considered as effective electron donor to capture the photo-generated h^+ for preventing recombination of e^-/h^+ pairs, obtaining enhanced and high stable photocurrent response.

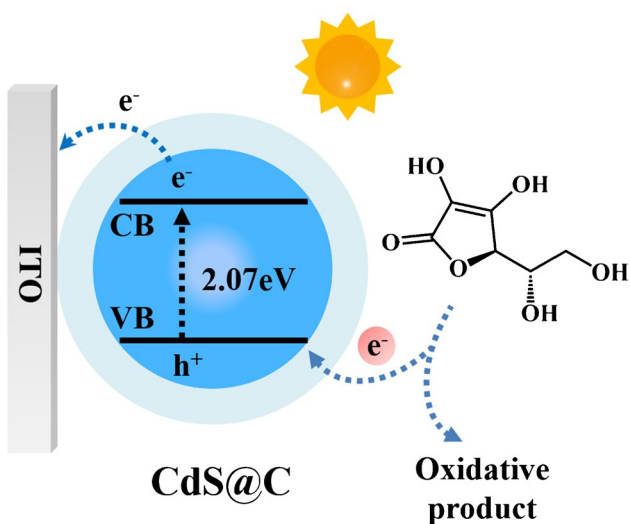## Optimization of experimental conditions

To achieve excellent analytical performance of PEC aptamer sensor, several main experimental parameters were optimized (Fig. S1, ESM). The experimental results show that the optimal CdS@C NR-loaded concentration is 2.0 mg mL^{-1}; the optimal E2 incubation time is 40 min; and the optimal pH of PBS is 8.0. Then, the above parameters
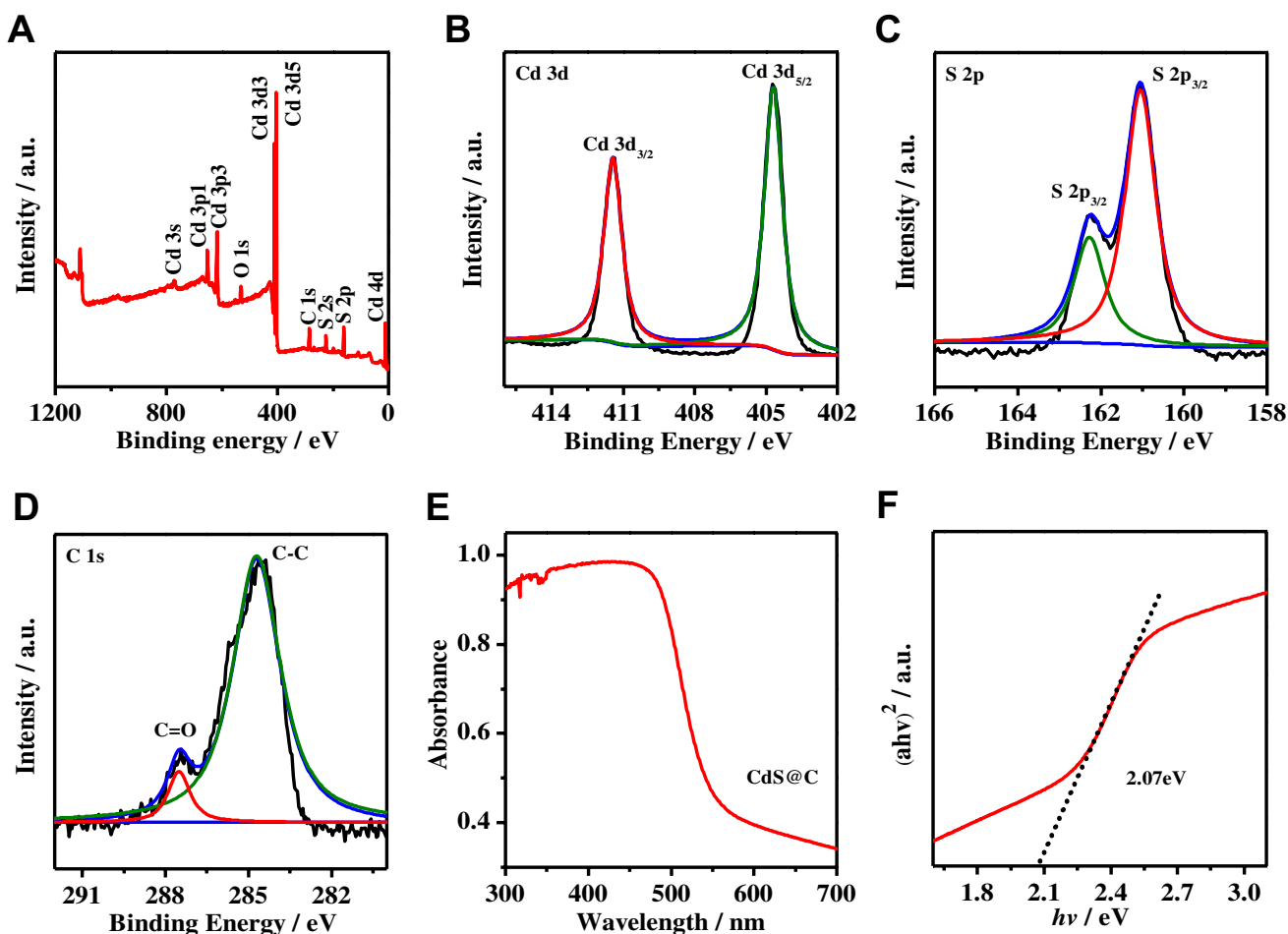
Fig. 2 **A** Survey XPS spectrum. **B–D** High-resolution Cd 3d, S 2p, and C 1 s XPS spectra. **E** UV–vis diffuse reflectance spectra. **F** The band gap energy of CdS@C NRs


Scheme 2 Possible charge-transfer mechanism in CdS@C NRs under light illumination (CB, conduction band; VB, valence band)

were chosen for the subsequent experiments. The specific experimental results are provided in ESM.

Analytical performance of the developed PEC aptasensor

To demonstrate the feasibility, the construction process of the aptasensor was studied through the PEC response and electrochemical impedance spectroscopy (EIS). As shown in Fig. 3A, an obvious photocurrent response can be observed after the introduction of CdS@C NRs (curve a). When CS (curve b), ssDNA (curve c), BSA (curve d), and ALP-apta (curve e) are successively modified on the electrode surface, the photocurrent will decrease gradually owing to the introduction of non-conductive substances, such as aptamers, proteins, and polymer. With the addition of analyte E2 (curve f), the photocurrent could return to a certain extent, which may be caused by the release of the formed E2-apta conjugate from the electrode surface.
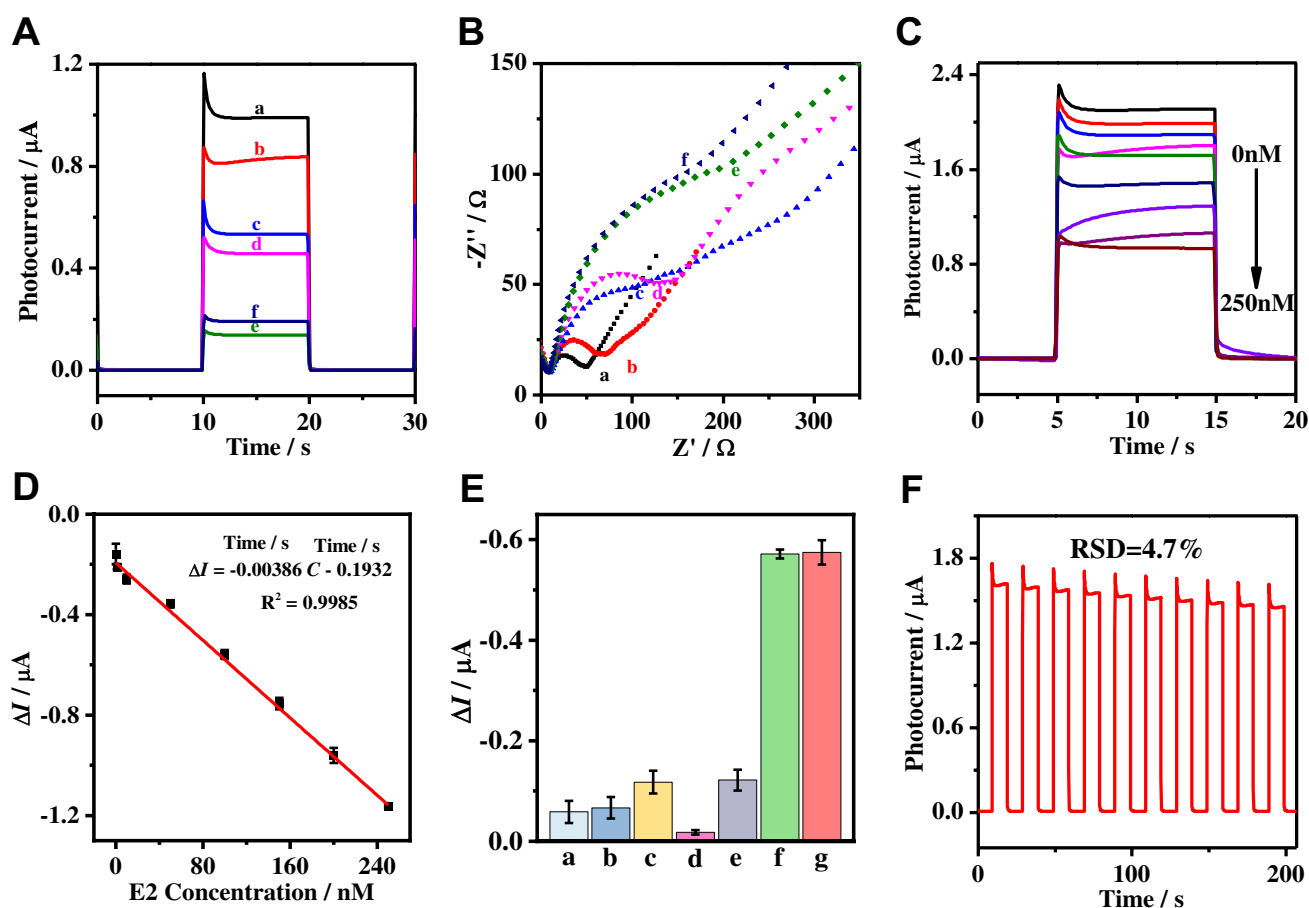
Fig. 3 **A–B** Photocurrent response, and the corresponding EIS spectra of the CdS@C NRs/ITO (curve a), CS/CdS@C NRs/ITO (curve b), ssDNA/CS/ CdS@C NRs/ITO (curve c), BSA/ssDNA/CS/CdS@C NRs/ITO (curve d), ALP-apta/BSA/ssDNA/CS/CdS@C NRs/ITO (curve e), and E2/ALP-apta/BSA/ssDNA/CS/CdS@C NRs/ITO (curve f). **C** Photocurrents of the aptasensor with various con-centrations of E2 from 0 to 250 nM. (D) The corresponding calibration plots. **E** Specificity of the developed aptasensor against 100 nM E2 (f), 100-fold bisphenol A (a), nonyl phenol (b), ethinylestradiol (c), atrazine (d), ciprofloxacin (e), and a mixture (containing all the analytes, g). **F** Stability of the proposed aptasensor, $C_{E2} = 100$ nM (error bar = standard deviation, $n = 3$)

EIS was further carried out to characterize the electro-chemical properties of the aptasensor during stepwise reactions (Fig. 3B), which were measured at the applied potential of 0.241 V in the frequency range from 0.1 to 100 kHz in 0.1 M KCl solution containing 5.0 mM $[Fe(CN)_6]^{3-/4-}$. With the immobilization of CS (curve b), ssDNA (curve c), BSA (curve d), and ALP-apta (curve e) on the CdS@C NRs/ITO (curve a) surface, the charge transfer resistance (Rct) gradually increases causing by the non-conductivity of introduced biomolecules. Following the addition of E2, the Rct declines (curve f), because a E2-ALP-apta conjugate is formed and dislodged from the electrode surface. In addition, the gel electrophoresis experiment was carried to further verify the construction principle of our proposed aptasensor (Fig. S2, ESM). These above results demonstrate the successful construction of the aptasensor.

To evaluate the analytical performance, the proposed PEC aptasensor was explored against diverse concentrations of E2 under the optimized conditions. Figure 3C displays that the photocurrents gradually decrease with the E2 concentrations from 0 to 250 nM, because of the decrease of in situ produced AA by the ALP enzymatic catalysis. Meanwhile, a good linear relationship was achieved between the photocurrent change value ΔI ($\Delta I = I - I_0$) and the concentration of E2 from 1.0 to 250 nM with the detection limit of 0.37 nM (Fig. 3D), and the linear regression equation is ΔI (μA) $= -0.00386 \, C_{E2} - 0.1932$, with a correlation coefficient (R^2) of 0.9985. The obtained results exhibited comparable or even better analytical performance for E2 determination in contrast with the obvious reported work (Table S1, ESM) [6, 30–35].

Specificity and stability of the fabricated sensor

To investigate the selectivity of the PEC aptasensor, the PEC signals were recorded against the 100 nM E2, and several

10 µM interfering substances, including bisphenol A, nonyl phenol, ethinylestradiol, atrazine, ciprofloxacin, and mixture (Fig. 3E). The concentration of interferents is 100-fold than that of the target (E2), so the non-specific is inevitable. And the chemical structure of ethinylestradiol and ciprofloxacin among these interferents are more similar with E2; hence, the interference signal is relatively large. However, the photoelectrochemical response signal of the mixture (include 100 nM analyte and 10 µM all the interferents, column f in Fig. 3E) is almost identical in comparison with 100 nM pure analyte (column g in Fig. 3E), which further demonstrates the high selectivity of the prepared aptasensor for E2 detection. Then, the photocurrent at 100 nM E2 was detected to assess the stability of aptasensor within 210 s (Fig. 3F). There is no obvious photocurrent variation with the relative standard deviation (RSD) of 4.7% during the testing process, indicating the excellent stability of the constructed aptasensor.

Precision was vital for the proposed PEC aptasensor, which can be evaluated via its reproducibility. The reproducibility was measured by five independent aptasensor at different E2 concentrations (50 nM, 100 nM, and 150 nM E2) with the RSD of 0.91%, 0.92%, and 1.63%, respectively. The result confirms the acceptable repeatability of the PEC aptasensor.

Real sample assay

Utility and reliability of the PEC aptasensor was conducted through standard addition method in the real samples' analysis. A total of 50 nM, 100 nM, and 150 nM E2 were separately added to the tap water and human serum samples to calculate the recoveries of the spiked amount of E2. The tap water and human serum samples were respectively obtained from laboratory water pipes and Jinhua Municipal Central Hospital Medical Group. Table 1 exhibits the recoveries of E2 analysis in the real samples. The recoveries are in the range of 99.10 ~ 102.43% with the RSDs of 0.42 ~ 2.01% ($n = 3$), revealing the feasibility and potential utility of the developed aptasensor in environmental samples analysis.

Table 1 Detection of E2 in tap water at different concentrations ($n = 3$)

Samples	Added (nM)	Found (nM)	Recovery (%)	RSD (%)
Tap water	50.00	50.66 ± 0.21	101.32	0.42
	100.00	99.80 ± 1.17	99.79	1.17
	150.00	150.23 ± 1.38	100.15	0.92
Human serum	50.00	50.11 ± 1.05	100.22	1.53
	100.00	102.43 ± 1.26	102.43	0.96
	150.00	148.65 ± 0.83	99.10	2.01

Conclusions

In this work, an ultrasensitive signal-off PEC aptasensor for the E2 detection was developed by integrating the prepared CdS@C NRs as photoactive substance and enzyme-mediated signal amplification strategy. The developed PEC aptasensor has a relatively wide linear range of 1.0 ~ 250 nM and low LOD of 0.37 nM. Although the present work has achieved satisfactory results and expanded the possibilities of sensitive analysis of other environmental pollutants, the development of photoinductive sensors still faces some challenges, such as the design of ideal photoactive materials, lower detection limits, and higher specificity.

Declarations

Conflict of interest The authors declare no competing interests.

References

1. Adeel M, Song X, Wang Y, Francis D, Yang Y (2017) Environmental impact of estrogens on human, animal and plant life: a critical review. Environ Int 99:107–119. https://doi.org/10.1016/j.envint.2016.12.010
2. Li Y, Liu L, Feng J, Ren X, Zhang Y, Yan T, Liu X, Wei Q (2020) A self-powered photoelectrochemical cathodic aptasensor for the detection of 17β-estradiol based on FeOOH/In$_2$S$_3$ photoanode. Biosens Bioelectron 154:112089. https://doi.org/10.1016/j.bios.2020.112089
3. Jan van Winden L, Kok M, Acda M, Dezentje V, Linn S, Shi R-Z, van Rossum HH (2021) Simultaneous analysis of E1 and E2 by LC-MS/MS in healthy volunteers: estimation of reference intervals and comparison with a conventional E2 immunoassay. J Chromatogr B 122563. https://doi.org/10.1016/j.jchromb.2021.122563
4. Minopoli A, Sakač N, Lenyk B, Campanile R, Mayer D, Offenhäusser A, Velotta R, Della Ventura B (2020) LSPR-based colorimetric immunosensor for rapid and sensitive 17β-estradiol detection in tap water. Sens Actuators, B 308:127699. https://doi.org/10.1016/j.snb.2020.127699
5. Chaisuwan N, Xu H, Wu G, Liu J (2013) A highly sensitive differential pulse anodic stripping voltammetry for determination of 17β-estradiol (E2) using CdSe quantum dots based on indirect competitive immunoassay. Biosens Bioelectron 46:150–154. https://doi.org/10.1016/j.bios.2013.02.041
6. Ming W, Wang X, Lu W, Zhang Z, Song X, Li J, Chen L (2017) Magnetic molecularly imprinted polymers for the fluorescent detection of trace 17β-estradiol in environmental water. Sens Actuators, B 238:1309–1315. https://doi.org/10.1016/j.snb.2016.09.111

7. Singh AC, Asif M, Bacher G, Danielsson B, Willander M, Bhand S (2019) Nanoimmunosensor based on ZnO nanorods for ultrasensitive detection of 17β-Estradiol. Biosens Bioelectron 126:15–22. https://doi.org/10.1016/j.bios.2018.10.004

8. Yao X, Gao J, Yan K, Chen Y, Zhang J (2020) Ratiometric self-powered sensor for 17β-estradiol detection based on a dual-channel photocatalytic fuel cell. Anal Chem 92(12):8026–8030. https://doi.org/10.1021/acs.analchem.0c01543

9. Zhao WW, Xu JJ, Chen HY (2017) Photoelectrochemical enzymatic biosensors. Biosens Bioelectron 92:294–304. https://doi.org/10.1016/j.bios.2016.11.009

10. Zhang Z, Liu Q, Zhang M, You F, Hao N, Ding C, Wang K (2021) Simultaneous detection of enrofloxacin and ciprofloxacin in milk using a bias potentials controlling-based photoelectrochemical aptasensor. J Hazard Mater 416:125988. https://doi.org/10.1016/j.jhazmat.2021.125988

11. Cao J-T, Lv J-L, Liao X-J, Ma S-H, Liu Y-M (2021) Photogenerated hole-induced chemical–chemical redox cycling strategy on a direct Z-scheme Bi_2S_3/Bi_2MoO_6 heterostructure photoelectrode: toward an ultrasensitive photoelectrochemical immunoassay. Anal Chem. https://doi.org/10.1021/acs.analchem.1c02175

12. Li H, Han M, Weng X, Zhang Y, Li J (2021) DNA-tetrahedral-nanostructure-based entropy-driven amplifier for high-performance photoelectrochemical biosensing. ACS Nano 15(1):1710–1717. https://doi.org/10.1021/acsnano.0c09374

13. Zhou Q, Tang D (2020) Recent advances in photoelectrochemical biosensors for analysis of mycotoxins in food. TrAC, Trends Anal Chem 124:115814. https://doi.org/10.1016/j.trac.2020.115814

14. Yang H, Xu M, Li Z, Ge S, Zhang L, Zhu P, Yu J (2020) Dual-photocathode array propelled lab-on-paper ratiometric photoelectrochemical sensing platform for ultrasensitive microRNA bioassay. Sens Actuators, B 316. https://doi.org/10.1016/j.snb.2020.128093

15. Yang H, Zhang M, Wang L, Yu R, Tu W, Wang Z, Wang R, Gao H, Dai Z (2021) Modulating polarization of perovskite-based heterostructures via in situ semiconductor generation and enzyme catalysis for signal-switchable photoelectrochemical biosensing. Anal Chem. https://doi.org/10.1021/acs.analchem.1c01457

16. Long D, Li M, Wang H, Wang H, Chai Y, Li Z, Yuan R (2020) Ultrasensitive photoelectrochemical assay for DNA detection based on a novel SnS_2/Co_3O_4 sensitized structure. Anal Chem 92(21):14769–14774. https://doi.org/10.1021/acs.analchem.0c03497

17. Li Z, Su C, Wu D, Zhang Z (2018) Gold nanoparticles decorated hematite photoelectrode for sensitive and selective photoelectrochemical aptasensing of lysozyme. Anal Chem 90(1):961–967. https://doi.org/10.1021/acs.analchem.7b04015

18. Han SC, Pu YC, Zheng LX, Hu LF, Zhang JZ, Fang XS (2016) Uniform carbon-coated CdS core-shell nanostructures: synthesis, ultrafast charge carrier dynamics, and photoelectrochemical water splitting. J Mater Chem A 4(3):1078–1086. https://doi.org/10.1039/C5TA09024E

19. Hu Y, Gao X, Yu L, Wang Y, Ning J, Xu S, Lou XW (2013) Carbon-coated CdS petalous nanostructures with enhanced photostability and photocatalytic activity. Angew Chem Int Ed 52(21):5636–5639. https://doi.org/10.1002/anie.201301709

20. Zou S, Fu Z, Xiang C, Wu W, Tang S, Liu Y, Yin D (2015) Mild, one-step hydrothermal synthesis of carbon-coated CdS nanoparticles with improved photocatalytic activity and stability. Chin J Catal 36(7):1077–1085. https://doi.org/10.1016/S1872-2067(15)60827-0

21. Tian J, Huang T, Lu J (2016) A photoelectrochemical aptasensor for mucin 1 based on DNA/aptamer linking of quantum dots and TiO$_2$ nanotube arrays. Anal Methods 8(11):2375–2382. https://doi.org/10.1039/C5AY02290H

22. Zhu JH, Feng YG, Wang AJ, Mei LP, Luo X, Feng JJ (2021) A signal-on photoelectrochemical aptasensor for chloramphenicol assay based on 3D self-supporting AgI/Ag/BiOI Z-scheme heterojunction arrays. Biosens Bioelectron 181:113158. https://doi.org/10.1016/j.bios.2021.113158

23. Li X, Zhu L, Zhou Y, Yin H, Ai S (2017) Enhanced photoelectrochemical method for sensitive detection of protein kinase A activity using TiO$_2$/g-C$_3$N$_4$, PAMAM dendrimer, and alkaline phosphatase. Anal Chem 89(4):2369–2376. https://doi.org/10.1021/acs.analchem.6b04184

24. Tang S, Xia Y, Fan J, Cheng B, Yu J, Ho W (2021) Enhanced photocatalytic H$_2$ production performance of CdS hollow spheres using C and Pt as bi-cocatalysts. Chin J Catal 42(5):743–752. https://doi.org/10.1016/S1872-2067(20)63695-6

25. Sun J, Yin M, Li Y, Liang K, Fan Y, Li Z (2021) Efficient photocatalytic hydrogen production of ternary composite constituted by cubic CdS, MoS$_2$ and activated carbon. J Alloys Compd 874:159930. https://doi.org/10.1016/j.jallcom.2021.159930

26. Sun R-M, Zhang L, Feng J-J, Fang K-M, Wang A-J (2022) In situ produced Co$_9$S$_8$ nanoclusters/Co/Mn-S, N multi-doped 3D porous carbon derived from eriochrome black T as an effective bifunctional oxygen electrocatalyst for rechargeable Zn-air batteries. J Colloid Interface Sci 608:2100–2110. https://doi.org/10.1016/j.jcis.2021.10.144

27. Zhu J-H, Wang M, Tu L-H, Wang A-J, Luo X, Mei L-P, Zhao T, Feng J-J (2021) Nanosheets-assembled hollow CdIn$_2$S$_4$ microspheres-based photoelectrochemical and fluorescent dual-mode aptasensor for highly sensitive assay of 17β-estradiol based on magnetic separation and enzyme catalytic amplification. Sens Actuators, B 130553. https://doi.org/10.1016/j.snb.2021.130553

28. Wu Y, Wang H, Tu W, Wu S, Liu Y, Tan YZ, Luo H, Yuan X, Chew JW (2018) Petal-like CdS nanostructures coated with exfoliated sulfur-doped carbon nitride via chemically activated chain termination for enhanced visible-light–driven photocatalytic water purification and H$_2$ generation. Appl Catal, B 229:181–191. https://doi.org/10.1016/j.apcatb.2018.02.029

29. Xing RZ, Li JX, Yang XG, Chen ZW, Huang R, Chen ZX, Zhou SG, Chen Z (2020) Preparation of high-performance CdS@C catalyst using Cd-enriched biochar recycled from plating wastewater. Front Chem 8:140. https://doi.org/10.3389/fchem.2020.00140

30. Wong A, Santos AM, Fava EL, Fatibello Filho O, Sotomayor MDPT (2019) Voltammetric determination of 17β-estradiol in different matrices using a screen-printed sensor modified with CuPc, Printex 6L carbon and Nafion film. Microchem J 147:365–373. https://doi.org/10.1016/j.microc.2019.03.052

31. Li Y, Zhao X, Li P, Huang Y, Wang J, Zhang J (2015) Highly sensitive Fe$_3$O$_4$ nanobeads/graphene-based molecularly imprinted electrochemical sensor for 17β-estradiol in water. Anal Chim Acta 884:106–113. https://doi.org/10.1016/j.aca.2015.05.022

32. Han Q, Shen X, Zhu W, Zhu C, Zhou X, Jiang H (2016) Magnetic sensing film based on Fe$_3$O$_4$@Au-GSH molecularly imprinted polymers for the electrochemical detection of estradiol. Biosens Bioelectron 79:180–186. https://doi.org/10.1016/j.bios.2015.12.017

33. Dong X, He L, Liu Y, Piao Y (2018) Preparation of highly conductive biochar nanoparticles for rapid and sensitive detection of 17β-estradiol in water. Electrochim Acta 292:55–62. https://doi.org/10.1016/j.electacta.2018.09.129

34. Wang W, Peng Y, Wu J, Zhang M, Li Q, Zhao Z, Liu M, Wang J, Cao G, Bai J, Gao Z (2021) Ultrasensitive detection of

17β-estradiol (E2) based on multistep isothermal amplification. Anal Chem 93(10):4488–4496. https://doi.org/10.1021/acs.analchem.0c04681

35. Lee M-H, Thomas JL, Su Z-L, Zhang Z-X, Lin C-Y, Huang Y-S, Yang C-H, Lin H-Y (2020) Doping of transition metal dichalcogenides in molecularly imprinted conductive polymers for the ultrasensitive determination of 17β-estradiol in eel serum. Biosens Bioelectron 150:111901. https://doi.org/10.1016/j.bios.2019.111901